ASIAN JOURNAL OF PHARMACEUTICAL AND CLINICAL RESEARCH

INNOVARE ACADEMIC SCIENCES
Knowledge to Innovation

Vol 19, Issue 2, 2026

Online - 2455-3891
Print - 0974-2441

Research Article

DESIGN, DEVELOPMENT, AND EVALUATION OF VILDAGLIPTIN-LOADED CROSSLINKED SODIUM ALGINATE AND MORINGA GUM MICROSPHERES BY IONOTROPIC GELATION METHOD AND *IN SILICO* STUDY USING PK-SIM SOFTWARE

SUDIPTA DAS*, SUDIPA MANDAL, SUPRABHA MANDAL, SOHAN SAHA, SAWAN DAS, RIMI DEY, BAISHALI GHOSH

Department of Pharmaceutics, Netaji Subhas Chandra Bose Institute of Pharmacy, Nadia, West Bengal, India.
***Corresponding author: Sudipta Das; Email: sudiptapharmacy6@gmail.com**

Received: 01 December 2025, Revised and Accepted: 22 December 2025

ABSTRACT

Objective: Vildagliptin, a widely used antidiabetic agent, requires multiple daily doses, which can compromise patient adherence. This study aimed to design, optimize, and evaluate sustained-release microspheres of Vildagliptin using sodium alginate and *Moringa* gum prepared by ionotropic gelation, with a focus on improving entrapment efficiency, swelling behavior, and controlled drug release. In addition, physiologically based pharmacokinetic (PBPK) modeling was performed to predict *in vivo* performance.

Methods: Microspheres were formulated using varying ratios of sodium alginate and *Moringa* gum. The polymers were dissolved in water at 50°C, followed by the incorporation of 100 mg of Vildagliptin. The mixture was dropped into barium chloride solutions of different concentrations to induce cross-linking, producing nine formulations. Formed microspheres were cured for 15 min, washed, and air-dried. All batches were evaluated for particle size, entrapment efficiency, swelling index, and *in vitro* drug-release behavior. Drug-release kinetics were analyzed using mathematical models, and PBPK simulations were conducted to assess predicted pharmacokinetic performance.

Results: Among the nine formulations, F7 exhibited the most desirable characteristics with the highest entrapment efficiency (31.39%), a swelling index of 88, and controlled drug release reaching 95% within 4 h. Kinetic studies showed that most batches followed the Korsmeyer-Peppas model, indicating diffusion-controlled sustained release. PBPK modeling further demonstrated that F7 provided prolonged therapeutic plasma levels compared to immediate-release patterns.

Conclusion: The study successfully developed sustained-release Vildagliptin microspheres using *Moringa* gum and barium chloride. Formulation F7 showed optimized entrapment, swelling capacity, and sustained-release performance, suggesting its potential to reduce dosing frequency and enhance patient compliance in diabetes management.

Keywords: Microspheres, Vildagliptin, Sodium alginate, *Moringa* gum, Ionotropic gelation, *In silico*; PBPK modeling.

 DOI: http://dx.doi.org/10.22159/ajpcr.2026v19i2.57676. Journal homepage: https://innovareacademics.in/journals/index.php/ajpcr

INTRODUCTION

Many drugs face challenges, such as low solubility, poor stability, or low bioavailability. This creates a clear need for safe, efficient delivery systems that can overcome the drawbacks of traditional treatments. The physiology of the gastrointestinal tract often limits how well conventional formulations work – especially for drugs that need to be absorbed in the lower intestine or colon. Standard dosage forms can't reliably handle gastric emptying or ensure targeted, sustained delivery to these distal regions [1]. An ideal drug delivery system should release the right amount of medication at the right time and target it to the correct site in the body, while maximizing the drug's activity and minimizing unwanted side effects [2]. Novel drug delivery systems have gained attention in recent years as they improve bioavailability, protect drugs from gastric degradation, allow site-specific delivery, reduce dosing frequency, and minimize side effects [3]. Microspheres are tiny, spherical particles that typically range in size from about 1–1000 µm. These microspheres can be made from a variety of materials, including both natural and synthetic polymers [4,5]. Vildagliptin is a novel, dual-acting Dipeptidyl peptidase-4 (DPP-4) inhibitor that effectively regulates endocrine responses during both hypoglycemic and hyperglycemic states. In addition to enhancing insulin sensitivity through better blood glucose control, Vildagliptin also improves insulin sensitivity by reducing glucagon secretion during meals. Its favorable therapeutic profile stems from the combined pancreatic and extra-pancreatic actions of the incretin hormones Glucagon-Like Peptide-1 and Gastric Inhibitory Polypeptide [6-8]. It is approved for use as a monotherapy or in combination with other antidiabetic agents for the treatment of type 2 diabetes mellitus. However, its therapeutic effectiveness is limited when delivered through conventional oral dosage forms due to its short elimination half-life of approximately 1.6–2.5 h and rapid metabolic clearance [9,10]. To address this issue, optimization enables the identification of conditions that ensure optimal drug performance and sustained release. Optimization in pharmaceutics refers to the systematic adjustment of formulation and process variables to achieve maximum therapeutic efficacy, stability, and patient compliance [11,12]. Developing an effective pharmaceutical formulation requires attaining the desired dissolution profile with minimal experimentation. Response Surface Methodology, grounded in the principles of Design of Experiments (DOE), is extensively used for the optimization of drug delivery systems. This approach enables systematic assessment of formulation and process variables and it facilitates accurate prediction of outcomes, better understanding of variable interactions, and efficient selection of the optimal formulation [13,14]. A factorial design studies the effect of multiple factors and their interactions on a response. In a three-level design, each factor is tested at low (−1), medium (0), and high (+1) levels, allowing evaluation of both linear and non-linear effects for better optimization and prediction. In a three-level factorial design, each factor is tested at three levels – commonly coded as low (−1), medium (0), and high (+1). This allows researchers

to explore both linear and non-linear (quadratic) relationships between factors and responses. Compared to two-level designs, three-level factorials provide better optimization and prediction of formulation performance [15,16].

Polymers play a crucial role in microsphere synthesis, as they allow the fabrication of uniformly shaped, well-defined particles across a broad size range [17]. Natural polymers are increasingly used in drug delivery formulations because they are highly biocompatible and biodegradable, making them safe and environmentally friendly [18,19]. Sodium alginate is well-known for forming gel-like structures in the presence of divalent cations, while *Moringa* gum, derived from *Moringa oleifera*, acts as a natural binder and release modifier. Alginates can be cross-linked using a range of physical and chemical methods. In chemically cross-linked gels, covalent bonds form between polymer chains, creating a more permanent and stable network. In contrast, physically cross-linked gels rely on non-covalent interactions – such as ionic bonding or hydrogen bonding – between polymer chains, resulting in a reversible and often less rigid structure [20,21]. *Moringa* gum, a natural exudate obtained from the stems of *M. oleifera*, has long been valued in both traditional Indian medicine and as a component of food and vegetables. The freshly released gum appears white but gradually changes to a reddish-brown or brownish-black color upon prolonged exposure to air. In the pharmaceutical and industrial sectors, *Moringa* gum has gained attention for its multifunctional properties. It is commonly used as a stabilizer, binder, mucoadhesive agent, disintegrant, and as a matrix for controlled and sustained drug release, making it a promising natural excipient in drug delivery systems [22,23]. With advances in computing power and greater access to pre-clinical, especially *in vitro*, ADME data, physiologically based pharmacokinetic (PBPK) modeling has gained significant attention in drug discovery and development. During the lead optimization stage, it can help predict human pharmacokinetics, including clinical doses and dosing schedules, making the development process more efficient [24]. A novel approach involves developing a PBPK model to predict how a drug behaves in human plasma using *in silico* simulations. The PK-Sim model was assessed for its ability to accurately forecast bioavailability and its potential role in streamlining drug discovery and development [25]. Microspheres offer several benefits over traditional drug delivery methods. They allow for controlled and targeted drug release, improves patient comfort and compliance. They also enhance the solubility of poorly water-soluble drugs, maintain steady plasma drug levels, and reduce the required dose, frequency, and side effects. It boosts bioavailability, improves stability, and extends the drug's half-life [26-28]. Microspheres have gained importance in drug delivery by enabling controlled release, improving bioavailability, and enhancing patient compliance. They are applied in areas, such as vaccine delivery, cancer therapy, ophthalmic treatments, and even gene delivery, offering targeted action with reduced side effects [29]. Emerging applications of microspheres include monoclonal antibody-mediated targeting, delivery through microparticulate carriers, vaccine delivery, topical administration using porous microspheres, and surface-modified microsphere systems [30]. The primary aim of this study was to design, formulate, and evaluate Vildagliptin-loaded microspheres using natural polymers – sodium alginate and *Moringa* gum – for sustained drug release, to enhance bioavailability and reduce dosing frequency in the management of Type II diabetes mellitus.

MATERIALS AND METHODS

Materials

Vildagliptin, sodium alginate, and *Moringa* gum were procured from Yarrow Chem Pvt. Ltd., Mumbai, India. Barium chloride ($BaCl_2$) was obtained from Nice Chemicals Pvt. Ltd., Cochin, India. As per the Certificate of Analysis, sodium alginate was of medium viscosity grade, and *Moringa* gum was a natural polysaccharide exudate with particle size below 250 µm and moisture content <10%. All chemicals and reagents used were of analytical grade and were used as received without further purification.

Instruments

During formulation, polymer solutions were stirred using a Magnetic Stirrer (LB-MS1, Labcare, India) at controlled speeds, and the temperature was maintained. Fourier-Transform Infrared (FTIR) spectra were recorded using an Alpha II-FTIR Spectrometer (Bruker, Germany) to assess drug-excipient compatibility. Surface morphology of the microspheres was examined using a Field Emission Scanning Electron Microscope, FE-SEM, Model JSM-7500F (JEOL, Japan). Drug content and *in vitro* release samples were analyzed using a ultraviolet (UV)-Visible Spectrophotometer (V-730, Jasco Inc., Japan) operated at 208 nm. The pH of buffer solutions was adjusted using a digital pH meter (LI 617, Elico Ltd., Chennai, India). Tobo USB Digital Microscope (Image Sensor: CMOS) is used for particle size determination. *In-vitro* drug release studies were performed using a USP Type II dissolution apparatus ("LABTRONICS" DISSOLUTION APPARATUS MODEL- LT-72 Mumbai, India) under sink conditions. PBPK simulations were conducted using PK-Sim® Software, Version 11.3.

Methodology

The method of ionotropic gelation (IG) was employed in the preparation of microspheres loaded with Vildagliptin by using biopolymers Sodium alginate and *Moringa* gum. IG works by crosslinking polyelectrolytes with counter-ions to form hydrogels. Natural polymers, such as alginate, gellan gum, chitosan, and carboxymethyl cellulose are commonly used to encapsulate drugs. In this process, polyvalent cations diffuse into drug-loaded polymer droplets, binding to anionic sites and creating a three-dimensional cross-linked network. The IG method is simple, cost-effective, and time-efficient, as it does not require sophisticated equipment or expensive reagents [31-33]. Barium chloride was used as cross-linking agents [34]. A 3^2 full factorial design was applied with two formulation variables:

Polymer ratio (Sodium alginate: *Moringa* gum) at three levels (low, medium, high).

Cross-linker concentration (Barium chloride) at three levels (1%, 2%, 3% w/v).

This is a 3^2 full factorial experimental design governing quantitative and *in vitro* analysis, along with *in silico* simulation studying various pharmacokinetics properties using PBPK Modeling.

This resulted in nine experimental batches (F1-F9). All formulations contained a fixed drug amount (100 mg), while only the polymer ratio and cross-linker concentration were varied.

A homogeneous solution was prepared by dissolving accurately required quantity of Sodium alginate in 15 mL of purified water by utilizing a magnetic stirrer(LB-MS1, Labcare, India), maintaining 200 rpm speed until it is dissolved. *Moringa* gum was also accurately weighed and dissolved in 15 mL purified warm water. The temperature of the above two solutions was maintained at 50°C. After complete dissolution, both the polymers were mixed uniformly.

In a different beaker, 100 mg of drug was mixed in 10 mL of water, and then the drug solution was added in the solution of polymers to form a drug polymer solution. In another beaker, counter-ion solution was prepared by adding different concentrations of barium chloride in 100 mL of purified water for different batches.

When the mixing was completed, the drug polymer solution was extruded by a flat-tipped needle into the counter-ion solution. In the counter-ion solution, the drug polymer droplets were permitted to stand for 15 min for the curing reaction to provide a spherical shape. Then prepared microspheres were strained using a mesh strainer and washed thoroughly with distilled water to remove the additional residue of cross-linking agents. Finally, microspheres were then placed on a Petri dish and dried at normal room temperature. The composition

of Vildagliptin loaded Microspheres of different formulations is shown in Table 1.

Characterization of Vildagliptin-loaded microspheres

FTIR analysis

FTIR spectroscopy (Bruker Germany - Alpha II FTIR) is a widely used technique for characterizing molecular structures through Infrared (IR) absorption bands. FTIR spectra were recorded in the range of 4000–400 cm^{-1} with a spectral resolution of 4 cm^{-1}, averaging 32 scans per sample. It enables the identification of functional groups, molecular bonding patterns, and interactions, providing valuable insights into polymer interfaces, natural fibers, and composite materials [35]. FTIR Spectroscopy was carried out to study about the chemical structure, chemical bonds, and different functional groups present in the drug and the excipients. The drug-excipient compatibility of the formulation prepared was also studied using FTIR analysis [36].

Surface morphology and particle size measurement

The external surface morphology of the microspheres was examined using scanning electron microscopy (SEM) (FE-SEM, Model JSM-7500F (JEOL, Japan). Samples were mounted directly onto SEM stubs using double-sided adhesive tape and subsequently coated with a 200 nm thick gold film under reduced pressure. Imaging was performed at an accelerating voltage of 10 KV [37]. A specified number of microspheres were randomly selected, and their sizes were measured using an optical microscope. The optical micrometer was calibrated using a standard stage micrometer to ensure accuracy. The mean diameter of the microspheres was then calculated for each batch [38].

Evaluation parameters

Percentage yield

The prepared microspheres were completely dried and then weighed. The percentage of yield is calculated by taking the weight of the initial drug and polymer, which are used in the preparation and the weight of the finally prepared microspheres. By using these two values, the percentage of yield can be calculated by this formula [39,40].

$$\text{Percentage of Yield} = \frac{\text{Weight of the microspheres}}{\text{Weight of the drug polymer}} \times 100$$

Determination of drug entrapment efficiency

Specified amounts of dried microspheres were properly weighed, crushed with a mortar-pestle, and were taken into the solution of phosphate buffer (pH 6.8) [41]. It is kept for a time period so that the time should allow the maximum release of the drug from the formulation. Then, the suspension was filtered and a sample was taken to be analyzed with an UV-Visible spectrophotometer (V- 730, Jasco Inc, Japan) at a wavelength of 208 nm.

$$\text{Drug entrapment efficiency} = \frac{X1}{X2} \times 100$$

Where, X1 = the experimental amount of the drug present in the beads, X2 = the theoretical amount of the drug taken initially [42,43].

Swelling index

This study was conducted in a buffer solution (pH 6.8). A 0.2 M KH_2PO_4 solution was prepared by dissolving 2.73 g in distilled water and adjusting the volume to 100 mL. A 0.2 M NaOH solution was prepared by dissolving 0.8 g in CO_2-free distilled water and making up to 100 mL. Phosphate buffer (pH 6.8) was obtained by mixing 25 mL of KH_2PO_4 solution with 11.2 mL of NaOH solution and diluting to 100 mL with distilled water, and adjusted to pH6.8 with the help of a pH meter (LI 617, Elico Ltd, Hyderabad, India) [44]. A pre-determined weight of the sample was accurately measured and dissolved in 100 mL of buffer medium, allowing it to swell for a specified period. At a pre-determined time, the swollen microspheres were carefully removed, blotted with tissue paper to remove surface moisture, and then weighed [45].

$$\text{Swelling Index} = \frac{\text{Final weight} - \text{Initial weight}}{\text{Initial weight}} \times 100$$

In vitro drug release study

The *in vitro* drug release from the microsphere was evaluated in distilled water using a USP Type II (rotating paddle) dissolution apparatus ("LABTRONICS" DISSOLUTION APPARATUS MODEL- LT-72, Mumbai, India) under sink conditions. A pre-weighed amount of each formulation was introduced into the dissolution medium [46].

At pre-determined time intervals, a 5 mL aliquot was withdrawn and immediately replaced with an equal volume of fresh dissolution medium to maintain constant volume and sink conditions. The collected samples were filtered and analyzed for absorbance at 208 nm using a UV–Visible spectrophotometer (V-730, Jasco Inc, Japan) with a suitable blank as reference [47,48]. All *in vitro* dissolution studies were carried out in triplicate (n = 3), and the results were expressed as mean±standard deviation.

Drug release kinetics

The drug release pattern of microspheres is depending upon the size, polymer density, cross-linking agents, polarity, pH of the medium, drug release through the matrix, and time. After collecting dissolution data, fitted in the popular release models, such as – Zero-order, First-order, Hixon-Crowell, and Korsemeyer-Peppas model to check the drug release kinetics and predict the overall release behavior of the drug through microspheres [49-51].

The mathematical models applied included:

Zero-order model ($Q = k_0 \cdot t + Q_0$), where drug release is constant over time. First-order model ($Q = Q_0 \cdot e^{(k_1 \cdot t)}$), where the release rate depends on the remaining drug. Higuchi model ($Q = k_H \cdot t^{0.5}$), which describes release as a diffusion process based on Fick's law. Hixson–Crowell model ($Q^{1/3} = k_{H\text{-}C} \cdot t + Q_0^{1/3}$), which considers changes in surface area and particle size as the drug dissolves. Korsmeyer–Peppas model ($Q = k_{K\text{-}P} \cdot t^n$), used especially when the release mechanism is not well defined or involves more than one process.

In the Korsmeyer-Peppas model, the release exponent (n) provides insights into the mechanism of drug release: If $n \leq 0.43$, it indicates Fickian diffusion (drug release controlled by diffusion). If $0.43 < n < 0.85$, it indicates non-Fickian or anomalous transport (a combination of

Table 1: Composition of Vildagliptin-loaded microspheres

Formulation code	Vildagliptin drug (mg)	Normalized levels of factors employed	
		Sodium alginate: *Moringa* Gum	Barium chloride (%W/V)
F1	100	1.00 (−1)	3.00 (+1)
F2	100	1.00 (−1)	2.00 (0)
F3	100	1.00 (−1)	1.00 (−1)
F4	100	2.50 (0)	3.00 (+1)
F5	100	2.50 (0)	2.00 (0)
F6	100	2.50 (0)	1.00 (−1)
F7	100	4 (+1)	3.00 (+1)
F8	100	4 (+1)	2.00 (0)
F9	100	4 (+1)	1.00 (−1)

Values represent the coded levels of formulation factors. Polymer ratio is expressed as Sodium Alginate: *Moringa* Gum at three factorial levels (−1, 0, +1), and cross-linker concentration represents Barium Chloride (% w/v) used for ionotropic gelation

diffusion and polymer relaxation). If n ≥ 0.85, the release follows Case-II transport, typically governed by polymer relaxation or swelling [52-54].

RESULTS AND DISCUSSION

DOE/Optimization

Optimization was performed based on a comparative evaluation of key response variables, including percentage yield, drug entrapment efficiency, swelling index, and cumulative drug release. A formal desirability function was not applied. Formulation F7 was selected as the optimized batch due to its superior overall performance across all evaluated parameters.

Characterization of Vildagliptin loaded microspheres

FTIR analysis

The FTIR spectrum of pure Vildagliptin shows characteristic functional group vibrations, including O–H/N–H stretching (3290 cm^{-1}), C–H stretching (2920–2850 cm^{-1}), and C=O stretching (1654 cm^{-1}). These peaks represent the intact molecular structure of the drug and serve as reference signatures for compatibility studies with polymers.

The spectrum highlights broad O–H stretching near 3355 cm^{-1}, typical of polysaccharides, along with a strong C–O stretching peak around 1015 cm^{-1}. Additional peaks in the 1600–1400 cm^{-1} region represent carbonyl and carboxylate functionalities inherent to natural gums. These characteristic vibrations confirm the presence of polymeric carbohydrate structures.

Fig. 1: Vildagliptin loaded crosslinked sodium alginate and *Moringa* gum microspheres

The absence of any significant peak shift, disappearance, or formation of new peaks in the FTIR spectrum of the optimized formulation (F7) compared to the pure drug confirms the absence of chemical interaction, indicating physical entrapment and excellent drug–polymer compatibility.

The prepared Vildagliptin-loaded crosslinked sodium alginate and Moringa gum microspheres are shown in Fig. 1, demonstrating their spherical morphology.

FT-IR analysis was performed using a FT-IR spectrometer. FTIR (Figs. 2-4) show wavenumber in cm^{-1} on X axis and transmittance [%] on Y axis. The FTIR spectrum in Fig. 2 shows prominent peaks at 3290 cm^{-1} (O–H/N–H stretching), 2920–2850 cm^{-1} (C–H stretching), and 1654 cm^{-1} (C=O stretching), indicating key functional groups. Peaks in the fingerprint region confirm the structural identity of the compound. From Fig. 3, it has been observed that the FTIR spectrum shows broad absorption around 3355 cm^{-1} (O–H stretching) and a strong peak at 1015 cm^{-1}, indicating C–O stretching of polysaccharides. Additional peaks in the 1600–1400 cm^{-1} range suggest the presence of C=O functional groups. From Fig. 4, the FTIR spectrum displays a broad peak around 3325 cm^{-1}, indicating O–H or N–H stretching, and a sharp peak at 1015 cm^{-1} corresponding to C–O stretching vibrations. Additional bands near 1640–1400 cm^{-1} suggest the presence of C=O and C=C functional groups. FTIR analysis revealed no interaction between the drug and polymer, confirming their compatibility.

Surface morphology and particle size

FE-SEM analysis was performed using JEOL MAKE, Model: JSM7500F. The surface morphology was studied under FE-SEM. From Fig. 5 the SEM images of Vildagliptin loaded microsphere shows a spherical shape with a rough, porous surface, and visible cracks, due to mechanical stress or excessive drying. The Figure shows a magnified image with a rough and highly porous surface, indicating a rough texture suitable for enhanced drug entrapment. The porous surface shows potential for controlled or sustained drug release.

FE-SEM images obtained at high magnification illustrate the external morphology of microspheres prepared through IG. The microspheres appear spherical with visibly rough and porous surfaces. The presence of pores and cracks suggests enhanced drug entrapment potential and controlled hydration behavior. Surface roughness indicates strong polymer cross-linking and supports sustained-release characteristics due to diffusional pathways within the matrix.

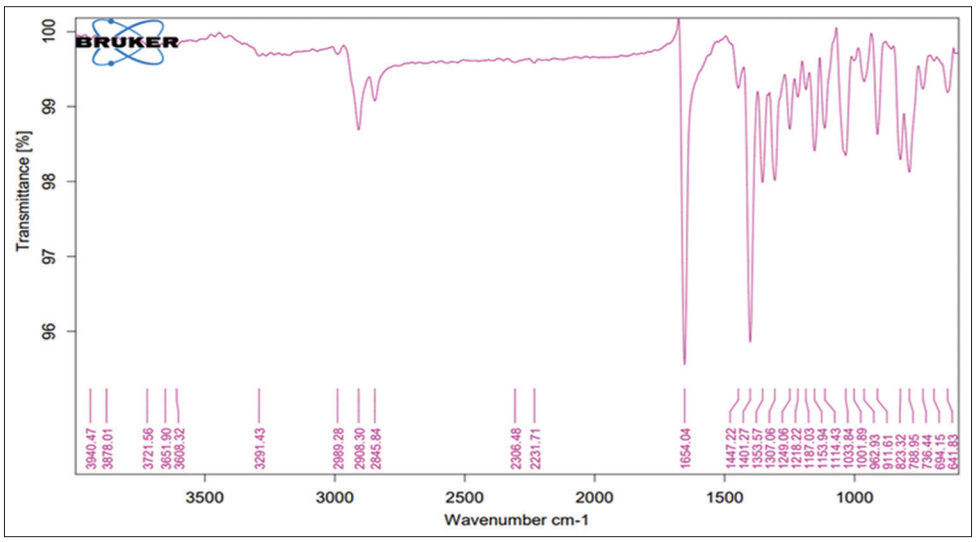

Fig. 2: Fourier-transform infrared graph of Vildagliptin

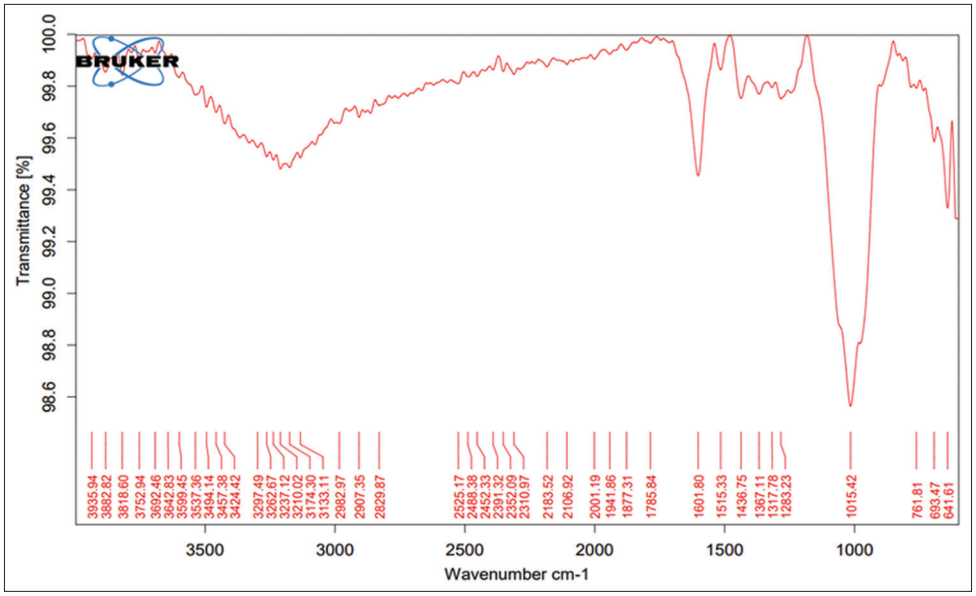

Fig. 3: Fourier-transform infrared graph of *Moringa* gum

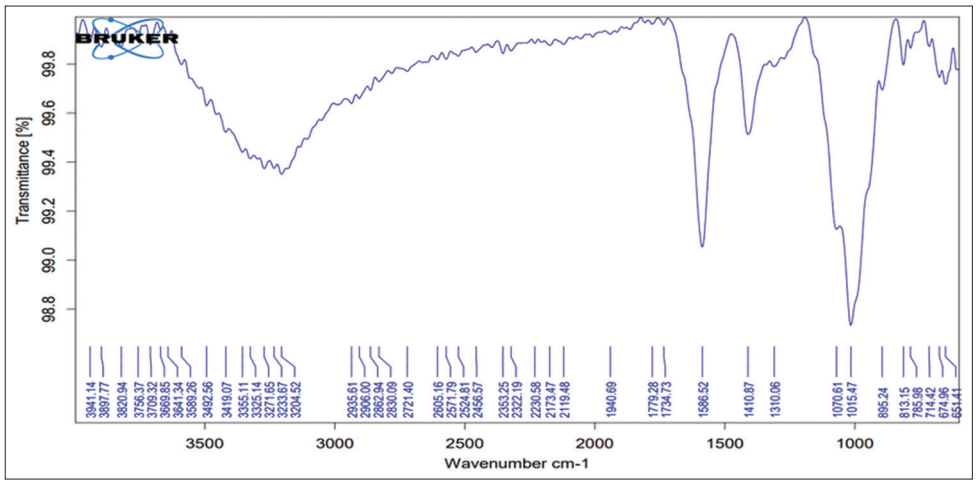

Fig. 4: Fourier-transform infrared graph of formulation (F7)

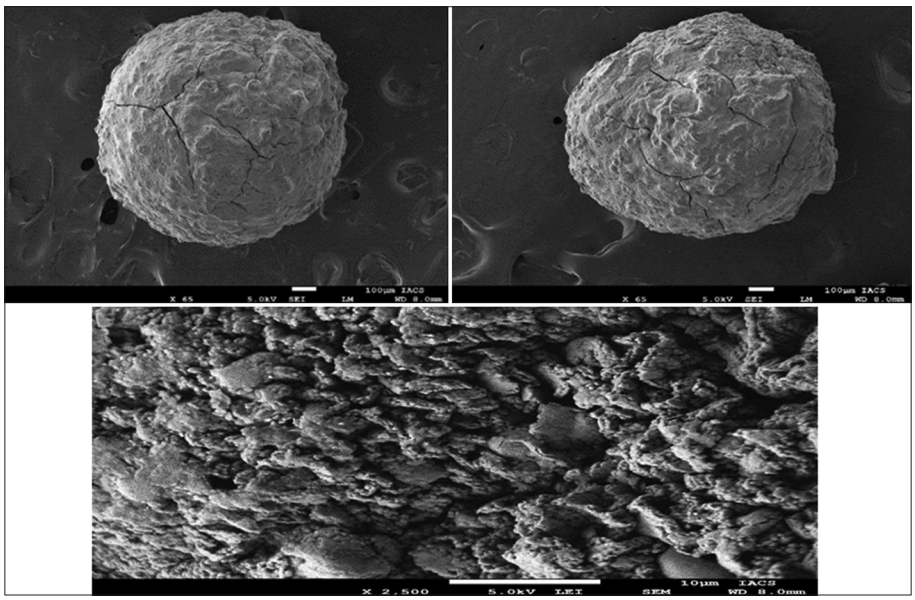

Fig. 5: Field emission scanning electron microscope images of Vildagliptin microspheres (F7)

Table 2: Particle size (Mean±SD) of the prepared 9 batches of microspheres

Formulation code	Particle size (mm) (Mean±SD)
F1	1.0±0.05
F2	0.9±0.04
F3	0.9±0.05
F4	0.8±0.03
F5	1.0±0.06
F6	1.0±0.05
F7	1.0±0.04
F8	1.0±0.05
F9	1.1±0.07

Particle size was measured using an optical microscope calibrated with a stage micrometre. SD indicates the standard deviation of measurements for each batch

Table 3: Percentage yield of prepared microspheres (Mean±SD, n=3)

Formulation code	Percentage yield (%)
F1	71.82±1.34
F2	68.18±1.12
F3	63.64±1.45
F4	90.91±1.08
F5	97.27±0.92
F6	98.18±0.85
F7	92.73±1.21
F8	97.27±0.89
F9	91.82±1.14

Values are expressed as Mean±SD (n=3)

The Particle size was determined using an optical microscope. From Table 2, the particle size of the formulations varies between 0.8 mm and 1.1 mm. Most batches (F1, F5 to F8) maintained a uniform size of 1.0 mm, with F4 showing the smallest particles (0.8 mm) and F9 exhibiting the largest (1.1 mm).

Result of evaluation parameters

Percentage yield

From Table 3, the percentage yield of the formulations ranged from 63.64% to 98.18%. The lowest yield was observed for F3 (63.64%), while the highest yield was recorded for F6 (98.18%), with most formulations showing yields above 90%, indicating efficient formulation processes. Fig. 6 shows the comparison graph of the percentage yield of Vildagliptin microspheres, with X-axis depicts Formulation Code of the prepared batches, and the Y-axis depicts Percentage yield of the prepared batches of Vildagliptin Microspheres.

Drug entrapment efficiency

From Table 4, the drug entrapment efficiency of the formulations ranged from 16.21% to 31.39%. The highest entrapment was observed in F7 (31.39%), while the lowest was in F5 (16.21%), indicating variation in the efficiency of drug incorporation among the formulations. Fig. 7, shows the comparison graph of drug entrapment efficiency of Vildagliptin microspheres, with X-axis depicts Formulation Code of prepared batches, and the Y-axis depicts drug entrapment efficiency of prepared batches of Vildagliptin Microspheres.

Swelling index

In Table 5, the swelling indices of the formulations ranged from 40 to 88. F1 exhibited the lowest swelling capacity (40) while F7 showed the highest swelling capacity (88), suggesting variations in the hydration and gel-forming ability of different formulations. Fig. 8, shows the comparison graph of the swelling index of Vildagliptin microspheres, with X- axis depicts Formulation Code of the prepared batches, and the Y-axis depicts Swelling Index of the prepared batches of Vildagliptin Microspheres.

Table 4: Drug entrapment efficiency of Vildagliptin microspheres (Mean ± SD, n = 3)

Formulation code	Drug entrapment efficiency (%)
F1	17.36 ± 0.78
F2	29.62 ± 1.05
F3	18.01 ± 0.82
F4	16.23 ± 0.69
F5	16.21 ± 0.73
F6	23.39 ± 0.91
F7	31.39 ± 0.98
F8	20.90 ± 0.87
F9	24.57 ± 0.94

Values are expressed as Mean ± SD (n = 3)

Table 5: Swelling index of Vildagliptin microspheres (Mean±SD, n=3)

Formulation code	Swelling index (%)
F1	40.0±1.56
F2	62.0±2.04
F3	55.0±1.87
F4	80.0±2.31
F5	53.0±1.92
F6	74.0±2.18
F7	88.0±2.14
F8	78.0±2.09
F9	63.0±1.96

Values are expressed as Mean±SD (n=3)

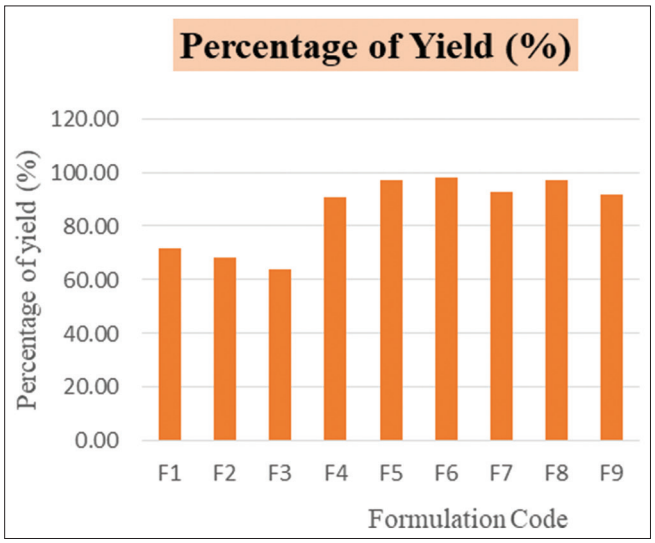

Fig. 6: Percentage yield comparison of Vildagliptin microsphere

In vitro drug release study

Fig. 9, shows the comparison graph of the drug release profile of Vildagliptin microspheres, with X-axis depicts Time in minutes, and the Y-axis depicts percentage of drug release of prepared batches of Vildagliptin Microspheres. It shows how different formulations (F1-F9) of Vildagliptin microspheres released the drug over time in a lab setup. Formulation F7 released the most drug, reaching about 95% by the end of the test, suggesting it may be the most effective for sustained delivery.

Drug release kinetics

The drug release behavior of the Vildagliptin-loaded microspheres was studied using various kinetic models to understand the mechanism behind the release. For formulation F7, the release exponent value (n=0.526) obtained from the Korsmeyer–Peppas model indicates

anomalous (non-Fickian) transport, confirming that drug release was governed by a combination of diffusion and polymer relaxation mechanisms. Among the five models tested – Zero-Order, First-Order, Higuchi, Hixson–Crowell, and Korsmeyer–Peppas – the Korsmeyer–Peppas model showed the best overall fit, especially for formulation F7, suggesting that the drug release was primarily governed by diffusion through the polymer matrix. The Higuchi model also fits many formulations well, indicating a significant diffusion-controlled release component. Meanwhile, the Hixson–Crowell model hinted at a role of erosion or reduction in particle size during the release process. The First-Order model showed good correlation for a few batches, pointing to a concentration-dependent release, while the Zero Order model, although ideal for sustained release, was less fitting for most formulations.

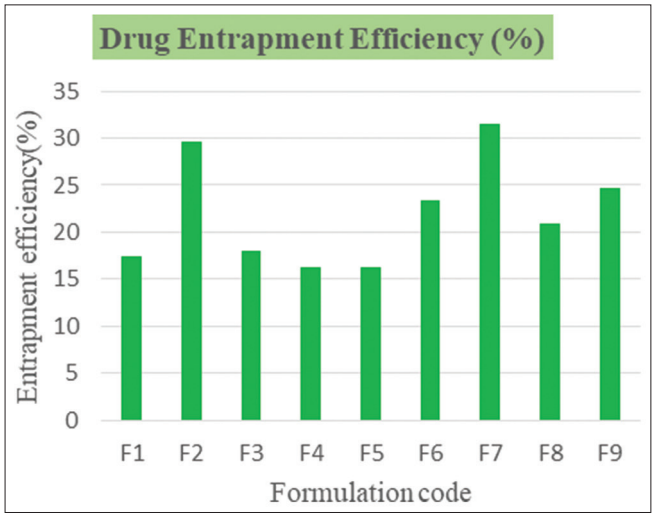

Fig. 7: Drug entrapment efficiency comparison of Vildagliptin

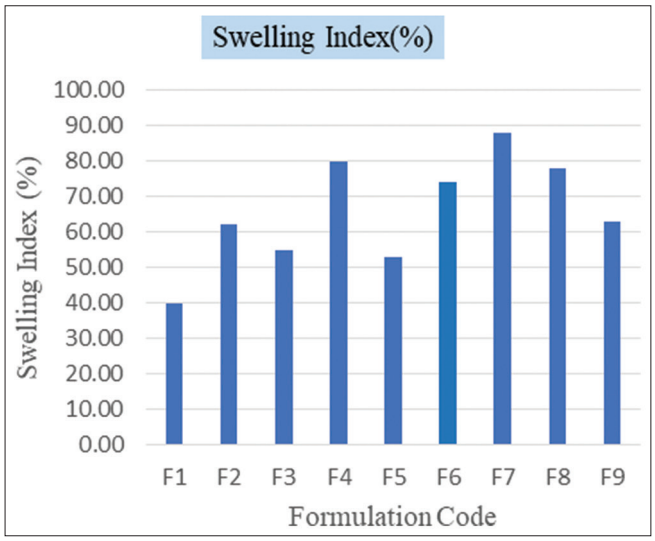

Fig. 8: Swelling behavior comparison of Vildagliptin microspheres

The regression coefficients (R^2) and release exponent (n) values obtained from different kinetic models for all formulations are summarized in Table 6.

PBPK modeling of Vildagliptin using PK-sim

PBPK modeling has emerged as a powerful quantitative framework for predicting drug absorption, distribution, metabolism, and excretion across diverse populations. By combining drug-specific physicochemical and pharmacokinetic properties with organism-level physiology, PBPK models enable mechanistic simulations of concentration–time profiles in plasma and tissues [55-58].

Model development and simulation

The PBPK model of vildagliptin, a selective DPP-4 inhibitor, was constructed in PK-Sim® - version 11.3, based on the drug's molecular characteristics and disposition parameters. The physicochemical parameter of drug profile – molecular weight: 303.4 g/mol, logP: 1.10, pKa: 9.03, water solubility ~ 1.15 mg/mL) and pharmacokinetic inputs, including plasma protein binding (fraction unbound: 90.70%) and renal clearance (13 L/h), were integrated into the model [59-62].

The model was initially compared and validated using previously published clinical data of oral administrations (100 mg) in healthy volunteers.

The clinical pharmacokinetic and pharmacodynamic profile of vildagliptin reported in humans was considered during PBPK model validation and comparison with published literature [63].

Administrative protocol of different formulations

PBPK-simulated plasma concentration curves compare the predicted systemic exposure of Vildagliptin after administration of different microsphere formulations. Higher plasma concentrations in optimized batches (e.g., F7) indicate slow and sustained drug availability, consistent with *in vitro* release behavior. Early peaks in some formulations reflect faster drug release and absorption.

The simulated blood plasma concentration–time profiles over the initial 4 h for all formulations are presented in Fig. 10, showing formulation-dependent differences in early drug absorption.

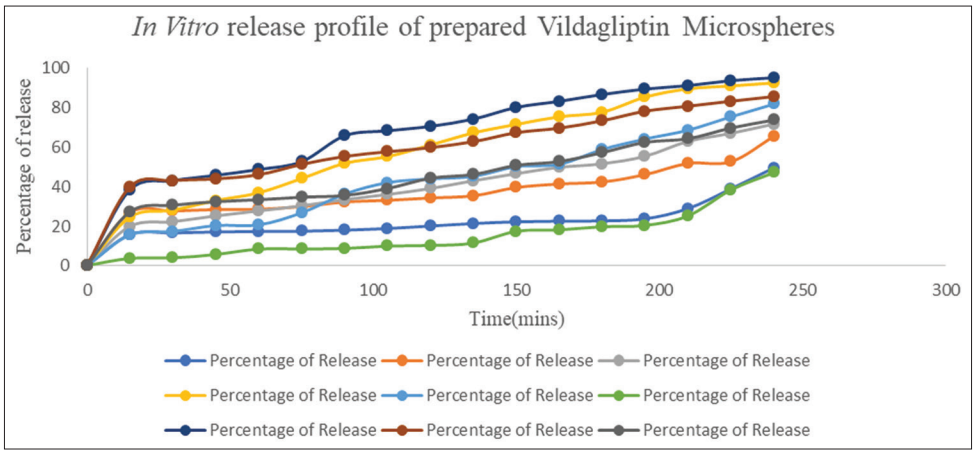

Fig. 9: Release profile of prepared Vildagliptin microspheres

The simulated blood plasma concentration values at corresponding time points for each formulation are provided in Table 8.

PBPK-analysis

PBPK analysis was carried out to evaluate the predicted in vivo pharmacokinetic behavior of Vildagliptin from the prepared microsphere formulations. The analysis involved the assessment of key pharmacokinetic parameters such as bioavailability, fraction absorbed, plasma clearance, maximum plasma concentration (C_max), time to reach maximum concentration (t_max), and mean residence time (MRT). The PBPK-simulated results indicated formulation-dependent variations in systemic drug exposure. Among all formulations, F7 demonstrated higher bioavailability, prolonged plasma concentration, and delayed drug elimination, which correlated well with the sustained *in vitro* drug release profile. These findings suggest that the optimized microsphere formulation is capable of maintaining therapeutic drug levels over an extended period.

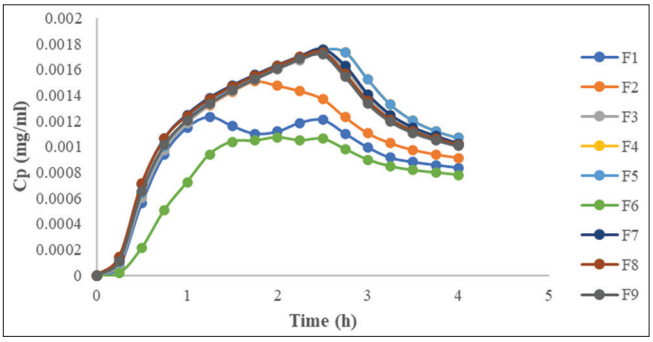

Fig. 10: Comparison of simulated blood plasma concentration in 4 h

The key pharmacokinetic parameters derived from PBPK analysis, including bioavailability, fraction absorbed, C_max, t_max, clearance, and mean residence time, are summarized in Table 9.

Simulation comparison using PKSim® software

The fraction of dose released at different time intervals for all formulations, as used in PBPK simulations, is presented in Table 7.

The 24-h PBPK simulation shows complete plasma concentration-time profiles for all formulations. Formulation F7 demonstrates prolonged therapeutic levels and delayed decline, confirming sustained-release behavior. The modeling integrates drug physicochemical parameters, *in vitro* release data, and physiological variables, providing predictive insights into *in vivo* pharmacokinetics.

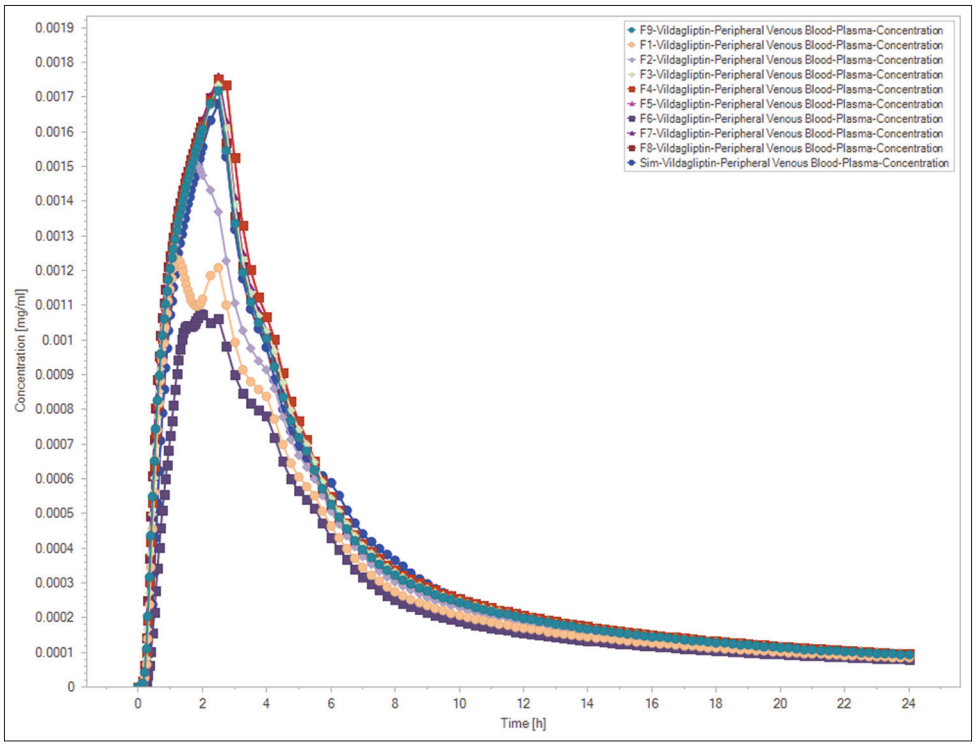

Fig. 11: Simulation comparison using PKSim® software where time taken 24 h

Table 6: Results of curve fitting of *in vitro* Vildagliptin release data from prepared batches of Vildagliptin loaded microsphere

Kinetic model	Regression co-efficient (R^2)								
	F1	F2	F3	F4	F5	F6	F7	F8	F9
Zero model	0.7143	0.8839	0.9623	0.965	0.9821	0.8194	0.8862	0.8602	0.9198
First model	0.667	0.8283	0.9436	0.9564	0.9238	0.7495	0.5535	0.9548	0.9339
Higuchi	0.6805	0.8616	0.9482	0.9833	0.9308	0.6751	0.9548	0.9565	0.9378
Hixon-Crowell	0.6851	0.9036	0.9653	0.9839	0.9568	0.7739	0.5463	0.9469	0.9401
Korsmeyer-Peppas	0.7916	0.8393	0.9587	0.9857	0.9034	0.6703	0.9802	0.9331	0.9479
n	0.2926	0.4449	0.443	0.4998	0.4885	0.4768	0.526	0.4707	0.472

R^2 values represent the goodness of fit for various kinetic models applied to the drug-release data. Release exponent (n) indicates the mechanism of drug diffusion based on the Korsmeyer-Peppas model

Table 7: Fraction of dose at different times

Time (h)	Fraction dose								
	F1	F2	F3	F4	F5	F6	F7	F8	F9
0	0	0	0	0	0	0	0	0	0
0.25	0.156	0.268	0.198	0.245	0.155	0.036	0.383	0.398	0.272
0.5	0.165	0.275	0.222	0.280	0.173	0.039	0.429	0.429	0.305
0.75	0.170	0.283	0.251	0.329	0.202	0.056	0.456	0.438	0.323
1	0.173	0.284	0.276	0.368	0.206	0.083	0.486	0.459	0.333
1.25	0.174	0.298	0.302	0.440	0.267	0.084	0.525	0.512	0.346
1.5	0.178	0.321	0.333	0.517	0.361	0.086	0.656	0.551	0.354
1.75	0.187	0.330	0.359	0.550	0.419	0.099	0.681	0.575	0.389
2	0.200	0.342	0.389	0.609	0.438	0.101	0.703	0.596	0.441
2.25	0.212	0.353	0.429	0.670	0.451	0.114	0.740	0.626	0.460
2.5	0.221	0.394	0.464	0.713	0.500	0.173	0.799	0.671	0.506
2.75	0.224	0.412	0.497	0.752	0.511	0.180	0.830	0.694	0.525
3	0.225	0.422	0.514	0.775	0.587	0.196	0.864	0.732	0.571
3.25	0.236	0.459	0.552	0.851	0.639	0.203	0.892	0.780	0.623
3.5	0.288	0.516	0.628	0.893	0.684	0.251	0.909	0.805	0.641
3.75	0.388	0.525	0.668	0.908	0.752	0.382	0.934	0.830	0.695
4	0.494	0.653	0.715	0.923	0.816	0.470	0.949	0.854	0.735

Table 8: Simulated blood plasma concentration (mg/mL) at different times

Time (h)	Fraction dose								
	F1	F2	F3	F4	F5	F6	F7	F8	F9
0	0	0	0	0	0	0	0	0	0
0.25	0.000066	0.000108	0.000083	0.000100	0.000100	0.000015	0.000139	0.000142	0.000109
0.5	0.000561	0.000648	0.000601	0.000636	0.000636	0.000214	0.000707	0.000713	0.000652
0.75	0.000940	0.001003	0.000974	0.001004	0.001004	0.000508	0.001063	0.001063	0.001013
1	0.001147	0.001193	0.001181	0.001210	0.001210	0.000723	0.001249	0.001241	0.001206
1.25	0.001232	0.001324	0.001326	0.001360	0.001360	0.000941	0.001380	0.001372	0.001338
1.5	0.001161	0.001430	0.001432	0.001460	0.001460	0.001040	0.001475	0.001469	0.001441
1.75	0.001101	0.001508	0.001521	0.001542	0.001542	0.001047	0.001557	0.001552	0.001527
2	0.001117	0.001474	0.001601	0.001619	0.001619	0.001073	0.001633	0.001629	0.001608
2.25	0.001185	0.001433	0.001674	0.001689	0.001689	0.001048	0.001702	0.001699	0.001682
2.5	0.001207	0.001371	0.001734	0.001753	0.001753	0.001061	0.001757	0.001737	0.001717
2.75	0.001102	0.001228	0.001609	0.001736	0.001736	0.000981	0.001629	0.001568	0.001544
3	0.000994	0.001106	0.001390	0.001524	0.001524	0.000899	0.001408	0.001356	0.001336
3.25	0.000914	0.001027	0.001232	0.001329	0.001329	0.000847	0.001248	0.001212	0.001195
3.5	0.000880	0.000976	0.001133	0.001202	0.001202	0.000817	0.001148	0.001123	0.001108
3.75	0.000858	0.000940	0.001069	0.001123	0.001123	0.000799	0.001083	0.001063	0.001051
4	0.000837	0.000914	0.001024	0.001068	0.001068	0.000781	0.001024	0.001017	0.001005

Table 9: Different parameters observed from PBPK analysis

Parameter	PBPK-analysis								
	F1	F2	F3	F4	F5	F6	F7	F8	F9
Bioavailability	0.059	0.065	0.068	0.071	0.070	0.054	0.072	0.069	0.068
Fraction Absorbed	0.051	0.057	0.061	0.064	0.063	0.045	0.065	0.062	0.061
Total Plasma Clearance (mL/min/kg)	165.14	151.12	139.39	136.12	137.12	180.94	139.83	140.42	141.95
C_max (µmol/l)	4.06	4.97	5.71	5.78	5.81	3.54	5.79	5.73	5.66
t_max (h)	1.25	1.80	2.50	2.50	2.50	1.95	2.50	2.50	2.50
MRT (h)	15.71	14.30	13.41	13.13	13.16	17.49	13.33	13.39	13.52

Among the tested formulations, F7 exhibited the most favorable pharmacokinetic profile, with the highest bioavailability (0.072) and fraction absorbed (0.065). It sustained plasma concentration and demonstrated an extended half-life of approximately 19 h. These results suggest that F7 achieved effective gastric retention and controlled drug release, likely due to optimized formulation parameters, such as polymer composition and matrix structure. The overall pharmacokinetic profiles indicate that these gastro-retentive formulations are capable of maintaining therapeutic plasma levels over an extended period, potentially allowing the reduced dosing frequency and improved patient adherence.

The complete 24-h PBPK-simulated plasma concentration–time profiles of all formulations are illustrated in Fig. 11, confirming the prolonged therapeutic exposure of formulation F7.

Statistical analysis

All experimental results were expressed as mean±standard deviation. Statistical comparison among different formulations was performed using one-way analysis of variance, followed by Tukey's *post hoc* test. Differences were considered statistically significant at $p<0.05$.

DISCUSSION

In this study, a factorial design approach was used to understand how changes in polymer concentration and cross-linker strength affect the properties of Vildagliptin-loaded microspheres. All nine formulations contained a fixed drug amount (100 mg), but the ratio of proportions of Sodium Alginate and *Moringa* Gum were varied at three levels – low (−1), medium (0), and high (+1). Similarly, the concentration of Barium Chloride as cross linking agent was also adjusted

at three levels, as shown in Table 1. By doing this, it was clearly observed how each variable – and their combinations – impacted key characteristics, such as drug entrapment, swelling ability, and the release behavior of the drug. This systematic approach helped identify the most effective combination (F7) for sustained release, offering better control over drug delivery. With decreasing Sodium Alginate to *Moringa* Gum ratio or increasing amount of *Moringa* gum in the microsphere formula, the drug release was found to be slower. This fact might be due to the hydrophilic property of *Moringa* gum. In fact, higher *Moringa* gum-containing microspheres were swelled more and might produce a viscous barrier over the microspheres. This viscous barrier might have produced a barrier to drug release from these microspheres. In addition, in most of the cases, the drug release was found to be sustained when the cross-linking concentration was in increasing order. Overall, the drug release was found to be sustained over 4 h. Among all the kinetic models studied, the Korsmeyer–Peppas model showed the best overall fit, especially for formulation F7, indicating that the drug release was mainly sustained by diffusion along with some polymer relaxation or erosion (non-Fickian behavior). The Higuchi and Hixson–Crowell models also showed a good fit for several formulations, suggesting that both diffusion through the matrix and gradual erosion of the microspheres contributed to the overall release pattern. In this study, PBPK modeling with PK-Sim® provided valuable insights into how the prepared vildagliptin microsphere formulations behave inside the body. By combining the drug's physicochemical properties with *in vitro* release data, the model was able to closely match clinical plasma concentration profiles reported in the literature. Among the tested batches, formulation F7 showed the most promising outcome, maintaining higher bioavailability and prolonged plasma levels compared to others. This suggests that the optimized microspheres could effectively overcome Vildagliptin's short half-life and support reduced dosing frequency. Overall, PBPK modeling proved to be a powerful approach for linking lab-based data with real biological performance, guiding the design of more patient-friendly sustained-release systems.

CONCLUSION

This experiment was performed with an objective to formulate and develop microspheres for control release of Vildagliptin by IG method, where barium chloride was used as a cross-linking agent and they were extensively evaluated in various parameters. The above study mainly focused on the effects of natural gum (*Moringa* gum) in the preparation of Vildagliptin microspheres. The evaluation has shown that the F7 batch has the highest swelling property, the F7 batch has the maximum drug entrapment efficiency, all the particle shapes are spherical in shape, and sizes were in between 0.1 and 1.0 mm (except batch F9, which has a size of 1.1 mm). In the *in vitro* release study, the F7 batch has shown the highest *in-vitro* release. The F4 batch has also shown better swelling behavior and *in-vitro* release compared to others. Among the nine formulations in the kinetic release study, the majority of them have maintained the Korsymeyer–Peppas model, which demonstrates the used microspheres were of swell able matrix type. From the results and discussion, it has been concluded that the drug diffusion from the Vildagliptin loaded Microsphere has maintained the sustained drug delivery system. The PBPK modeling clearly showed that the optimized vildagliptin microspheres, especially formulation F7, can maintain drug levels in the body for a longer time and improve overall bioavailability, suggesting its potential to achieve prolonged drug release based on *in vitro* and *in silico* performance.

ACKNOWLEDGMENT

The authors express their sincere gratitude to the principal and the management of Netaji Subhas Chandra Bose Institute of Pharmacy, Chakdaha, Nadia, West Bengal, for providing the necessary infrastructure and support to carry out this research work.

AUTHOR'S CONTRIBUTION

Study, Conception, and Design: Sudipta Das; Research work: Sudipa Mandal, Suprabha Mandal, Sohan Saha; Analysis and interpretation of results: Sawan Das, Rimi Dey, Baishali Ghosh.

AVAILABILITY OF DATA AND MATERIALS

All the data generated and analysed are included in this article.

ETHICS APPROVAL AND CONSENT TO PARTICIPATE

Not applicable.

CONFLICT OF INTEREST

The authors declare there is no conflict of interests.

FUNDING

The authors hereby declare there is no funding received for this study.

REFERENCES

1. Chauhan A, Gupta S, Singh P, Prasad Mishra G. Exploring the antidiabetic, lipid-lowering, and tissue repair benefits of multi-component microspheres in streptozotocin-induced diabetic rats. Asian J Pharm Clin Res. 2025 May;7:91-5. doi: 10.22159/ajpcr.2025v18i5.54330
2. Varde NK, Pack DW. Microspheres for controlled release drug delivery. Expert Opin Biol Ther. 2004 Jan;4(1):35-51. doi: 10.1517/14712598.4.1.35, PMID 14680467
3. Rai VK, Mishra N, Agrawal AK, Jain S, Yadav NP. Novel drug delivery system: An immense hope for diabetics. Drug Deliv. 2016 Sep 1;23(7):2371-90. doi: 10.3109/10717544.2014.991001, PMID 25544604
4. Sah SK, Vasia M, Yadav RP, Patel S, Sharma M. Microsphere overview. Asian J Pharm Res Dev. 2021;9(4):132-40. doi: 10.22270/ajprd.v9i4.1003
5. Mahale MM, Saudagar RB. Microsphere: A review. J Drug Deliv Ther. 2019 Jun;9(3-s):854-6. doi: 10.22270/jddt.v9i3-s.2826
6. Ahrén B, Schweizer A, Dejager S, Villhauer EB, Dunning BE, Foley JE. Mechanisms of action of the dipeptidyl peptidase-4 inhibitor vildagliptin in humans. Diabetes Obes Metab. 2011 Sep;13(9):775-83. doi: 10.1111/j.1463-1326.2011.01414.x, PMID 21507182
7. Foley JE. Insights into GLP-1 and GIP actions emerging from vildagliptin mechanism studies in Man. Front Endocrinol. 2019;10(10):780. doi: 10.3389/fendo.2019.00780, PMID 31781045
8. Schweizer A, Foley JE, Kothny W, Ahrén B. Clinical evidence and mechanistic basis for vildagliptin's effect in combination with insulin. Vasc Health Risk Manag. 2013 Feb 15;9:57-64. doi: 10.2147/VHRM.S40972, PMID 23431062
9. Manubolu K, Peeriga R. Formulation and *in-vitro* evaluation of vildagliptin microspheres using pectin and xanthan gum as polymers. Curr Indian Sci. 2025;3(1):e2210299X363340. doi: 10.2174/012210299X363340250116071643
10. He YL, Serra D, Wang Y, Campestrini J, Riviere GJ, Deacon CF, *et al*. Pharmacokinetics and pharmacodynamics of vildagliptin in patients with type 2 diabetes mellitus. Clin Pharmacokinet. 2007 Jul 1;46(7):577-88. doi: 10.2165/00003088-200746070-00003, PMID 17596103
11. Bezerra MA, Santelli RE, Oliveira EP, Villar LS, Escaleira LA. Response surface methodology (RSM) as a tool for optimization in analytical chemistry. Talanta. 2008 Sep 15;76(5):965-77. doi: 10.1016/j.talanta.2008.05.019, PMID 18761143
12. Uy M, Telford JK. Optimization by Design of Experiment Techniques IEEE Aerospace Conference, Big Sky, MT, USA; 2009. p. 1-10. doi: 10.1109/Aero.2009.4839625
13. Gupta SK, Patra S. Development, characterization and pharmacokinetic evaluation of optimized vildagliptin sustained release matrix tablet using box-Behnken design. Int J App Pharm. 2024 Jan;16(1):214-33. doi: 10.22159/ijap.2024v16i1.48052
14. Kuksal A, Tiwary AK, Jain NK, Jain S. Formulation and *in vitro*, *in vivo* evaluation of extended-release matrix tablet of zidovudine: Influence of the combination of hydrophilic and hydrophobic matrix formers. AAPS PharmSciTech. 2006 Jan 3;7(1):E1. doi: 10.1208/pt070101, PMID 16584139
15. Azouz L, Dahmoune F, Rezgui F, G'Sell C. Full factorial design optimization of anti-inflammatory drug release by PCL-PEG-PCL microspheres. Mater Sci Eng C Mater Biol Appl. 2016 Jan;58:412-9. doi: 10.1016/j.msec.2015.08.058, PMID 26478328
16. Jankovic A, Chaudhary G, Goia F. Designing the design of experiments (DOE) - an investigation on the influence of different factorial designs on the characterization of complex systems. Energy Build. 2021 Nov;250(2):111298. doi: 10.1016/j.enbuild.2021.111298
17. Saralidze K, Koole LH, Knetsch ML. Polymeric microspheres for medical applications. Materials. 2010 Jun 7;3(6):3537-64. doi: 10.3390/ma3063537
18. Nokhodchi A, Tailor A. *In situ* cross-linking of sodium alginate with calcium and aluminum ions to sustain the release of theophylline from polymeric matrices. Farmaco. 2004 Dec;59(12):999-1004. doi: 10.1016/j.farmac.2004.08.006, PMID 15598436

19. Kaplan DL, Wiley BJ, Mayer JM, Arcidiacono S, Keith J, Lombardi SJ, *et al*. In: Shalaby SW, editor. Biomedical Polymers. Vol. 5. New York: Hanser Publishers; 1994. p. 189-212. doi: 10.1002/pi.1995.210370114
20. Sachan NK, Pushkar S, Jha A, Bhattcharya AJ. Sodium alginate: The wonder polymer for controlled drug delivery. J Pharm Res. 2009 Aug;2(8):1191-9.
21. Lee KY, Mooney DJ. Alginate: Properties and biomedical applications. Prog Polym Sci. 2012 Jan;37(1):106-26. doi: 10.1016/j.progpolymsci.2011.06.003, PMID 22125349
22. Wang Q, Cui SW. Understanding the physical properties of food polysaccharides. Food Carbohydr Chem Phys Prop Appl. 2005;4(2):162-214. doi: 10.1201/9780203485286.ch4
23. Sonika SD, Singh TG, Arora G, Arora S. *Moringa* gum: A comprehensive review on its physicochemical and functional properties. Plant Arch. 2020;20:3794-805.
24. Zhuang X, Lu C. PBPK modeling and simulation in drug research and development. Acta Pharm Sin B. 2016 Sep;6(5):430-40. doi: 10.1016/j.apsb.2016.04.004, PMID 27909650
25. Cai H, Stoner C, Reddy A, Freiwald S, Smith D, Winters R, *et al*. Evaluation of an integrated *in vitro-in silico* PBPK (physiologically based pharmacokinetic) model to provide estimates of human bioavailability. Int J Pharm. 2006 Feb;308(1-2):133-9. doi: 10.1016/j.ijpharm.2005.11.002, PMID 16352407
26. Kakkar V, Wani SU, Gautam SP, Qadrie ZL. Role of microspheres in novel drug delivery systems: Preparation methods and applications. Int J Curr Pharm Sci. 2020 May;15(1):10-5. doi: 10.22159/ijcpr.2020v12i3.38326
27. Srivastava P, Visht S. Application and advancement of microsphere as controlled delivery system: A review. Int J Pharm Life Sci 2013;4:2583-94.
28. Virmani T, Gupta J. Pharmaceutical application of microspheres: An approach for the treatment of various diseases. Int J Pharm Sci Res. 2017;8(8):3253-60. doi: 10.13040/ijpsr.0975-8232.8(8).3252-60
29. Galande P, Yadav V, Borkar S. A review on microspheres: Preparation, characterization and applications. Asian J Pharm Res Dev. 2022 Dec 14;10(6):128-33. doi: 10.22270/ajprd.v10i6.1204
30. Patel NR, Patel DA, Bharadia PD, Pandya V, Modi D. Microsphere as a novel drug delivery. Int J Pharm Life Sci. 2011;2(8):945-51.
31. Patil JS, Kamalapur MV, Marapur SC. Kadam DV. Ionotropic gelation and polyelectrolyte complexation: The novel techniques to design hydrogel particulate sustained, modulated drug delivery system: A review. Digest J. Nanomat. Biostruct. 2010;5(1):241-8.
32. Pedroso-Santana S, Fleitas-Salazar N. Ionotropic gelation method in the synthesis of nanoparticles/microparticles for biomedical purposes. Polym Int. 2020 May;69(5):443-7. doi: 10.1002/pi.5970
33. Chechare DD, Siddaiah M. Formulation and evaluation of mucoadhesive microspheres of metronidazole. JAPR. 2024 Feb 29;12(1):93-9. doi: 10.18231/j.joapr.2024.12.1.93.99
34. Giridhar RS, Pandit AS. Effect of curing agent on sodium alginate blends using barium chloride as crosslinking agent and study of swelling, thermal, and morphological properties. Int J Polym Mater Polym Biomater. 2013 Jun;62(14):743-8. doi: 10.1080/00914037.2013.769236
35. Khan SA, Khan SB, Khan LU, Farooq A, Akhtar K, Asiri AM. Fourier transform infrared spectroscopy: Fundamentals and application in functional groups and nanomaterials characterization. In: Sharma SK, editor. Handbook of Materials Characterization. Cham: Springer; 2018. p. 317-44. doi: 10.1007/978-3-319-92955-2_9
36. Singh C, Rao K, Yadav N, Bansal N, Vashist Y, Kumari S, *et al*. A review: Drug excipient iincompatiblity by ftir spectroscopy. Curr Pharm Anal. 2023 Jun 1;19(5):371-8. doi: 10.2174/1573412919666230228102158
37. Rao DS, Reddy SH, Ramu S, Rambabu E. Preparation and evaluation of mucoadhesive microspheres of simvastatin by ionic gelation technique. Am J Adv Drug Deliv. 2014;2(5):594-608.
38. Das S, Dey R. Trivalent ion cross-linked and acetalated gellan gum microspheres of Glimepiride. Asian J Pharm Clin Res. 2020 Mar 9;13(5):66-8. doi: 10.22159/ajpcr.2020.v13i5.37229
39. Nayak AK, Khatua S, Hasnain MS, Sen KK. Development of diclofenac sodium-loaded alginate-PVP K 30 microbeads using central composite design. Daru. 2011;19(5):356-66. PMID 22615682
40. Mane S, Vinchurkar K, Khan MA, Sainy J. Effect of formulation variables on the characteristics of vildagliptin microspheres. IP Int J Comprehensive Adv Pharmacol. 2022 Aug 28;7(3):134-40. doi: 10.18231/j.ijcaap.2022.028
41. Devi S, Sharma K. Preparation and evaluation of ibuprofen loaded sodium alginate/sodium cmc mucoadhesive drug delivery system for sustained release. Actapharm. 2022;60(3):217. doi: 10.23893/1307-2080.APS.6015
42. Kesharvani S, Jaiswal PK, Mukerjee A, Singh AK. Formulation and evaluation of metformin hydrochloride loaded floating microspheres. Int J Pharm Pharm Sci. 2020;12(2):74-82. doi: 10.22159/ijpps.2020v12i2.35099
43. Viswanathan NB, Thomas PA, Pandit JK, Kulkarni MG, Mashelkar RA. Preparation of non-porous microspheres with high entrapment efficiency of proteins by a (water-in-oil)-in-oil emulsion technique. J Control Release. 1999 Mar 8;58(1):9-20. doi: 10.1016/S0168-3659(98)00140-0, PMID 10021485
44. Koreddi HA, Suryadevara VI, Talamanchi BA, Anne RA. Design and evaluation of bosentan controlled-release microcapsules. Int J Appl Pharm. 2022 Mar;14(2):87-94. doi: 10.22159/ijap.2022v14i2.43730
45. Datta A, Das A, Ghosh R. Eudragit® rl100 microspheres as delayed-release system for ibuprofen: *In vitro* evaluation. Int J Pharm Pharm Sci. 2022 Dec 1;4(2):6-10. doi: 10.22159/ijpps.2022v14i12.45838
46. Bhunia SN, Saha D, Das S, Dey R, Das S. Design, Formulation, and evaluation of hydrogel network based microbeads for prolonged release of valacyclovir. J Appl Pharma Res 2025;13:38-46. doi: 10.69857/joapr.v13i5.1668
47. Brahmaiah B, Desu PK, Nama S, Khalilullah S, Babu SS. Formulation and evaluation of extended release mucoadhesive microspheres of simvastatin. Int J Pharm Biomed Res. 2013;4(1):57-64.
48. Cherian AS, Boby Johns G, Praveen Raj R, Daisy PA, Jeny S. Formulation and evaluation of FSM-alginate beads of vildagliptin. J Drug Deliv Ther. 2019 Aug 30;9(4-A):246-51. doi: 10.22270/jddt.v9i4-A.3289
49. Bhasarkar J, Bal D. Kinetic investigation of a controlled drug delivery system based on alginate scaffold with embedded voids. J Appl Biomater Funct Mater. 2019 Apr;17(2):2280800018817462. doi: 10.1177/2280800018817462, PMID 31230497
50. Paarakh MP, Jose PA, Setty C, Peter GV. Release kinetics - concepts and applications. Int J Pharm Res Technol. 2018;8:12-2020.
51. Sivakumar M, Muthu Y, Elumalai K. Advancements in drug delivery systems: A focus on microsphere-based targeted delivery. Biomed Mater Devices. 2025 Sep 1;3(2):1030-57. doi: 10.1007/s44174-024-00245-6
52. Das S, Samanta A, Das S, Nayak AK. Sustained release of acyclovir from alginate-gellan gum and alginate-xanthan gum microbeads. JCIS Open. 2024 Apr;13:100106. doi: 10.1016/j.jciso.2024.100106
53. Jafari S, Soleimani M, Badinezhad M. Application of different mathematical models for further investigation of *in vitro* drug release mechanisms based on magnetic nano-composite. Polym Bull. 2022 Feb 1;79(2):1021-38. doi: 10.1007/s00289-021-03537-9
54. Medarametla RT, Gopaiah DK, Shaggir M, Raghavendra G, Reddy DN, Venkamma B. Drug release kinetics and mathematical models. Int J Pharm Sci Rev Res. 2024;27(9):24-6.
55. Rowland M, Peck C, Tucker G. Physiologically-based pharmacokinetics in drug development and regulatory science. Annu Rev Pharmacol Toxicol. 2011;51(1):45-73. doi: 10.1146/annurev-pharmtox-010510-100540, PMID 20854171
56. Jones HM, Parrott N, Jorga K, Lavé T. A novel strategy for physiologically based predictions of human pharmacokinetics. Clin Pharmacokinet. 2006;45(5):511-42. doi: 10.2165/00003088-200645050-00006, PMID 16640456
57. Kuepfer L, Niederalt C, Wendl T, Schlender JF, Willmann S, Lippert J, *et al*. Applied concepts in PBPK modelling: How to build a PBPK/PD model. CPT Pharmacometr Syst Pharmacol 2016;5(10):516-31. doi: 10.1002/psp4.12134
58. Rastogi R, Khatak P, Singh B. Alginate microspheres of isoniazid for oral sustained drug delivery: Formulation, characterization, and *in vitro* evaluation. J Microencapsul 2007;24(4):337-47.
59. Jones H, Rowland-Yeo K. Basic concepts in physiologically based pharmacokinetic modeling in drug discovery and development. CPT: Pharmacometrics Syst Pharmacol 2013;2(8):1-12. doi: 10.1038/psp.2013.41
60. Peters SA. Physiologically-based pharmacokinetic (PBPK) modeling and simulations: Principles, methods, and applications in the pharmaceutical industry. Hoboken (NJ): John Wiley and Sons; 2012. doi: 10.1002/9781118140291
61. Edginton AN, Schmitt W, Voith B, Willmann S. A mechanistic approach for the scaling of clearance in children. Clin Pharmacokinet. 2006;45(7):683-704. doi: 10.2165/00003088-200645070-00004, PMID 16802850
62. Willmann S, Höhn K, Edginton AN, Sevestre M, Solodenko J, Weiss W, *et al*. Development of a physiology-based whole-body population model for assessing the influence of individual variability on the pharmacokinetics of drugs. Clin Pharmacokinet. 2007;46(9):773-98. doi: 10.2165/00003088-200645100-00005
63. He YL. Clinical pharmacokinetics and pharmacodynamics of vildagliptin. Clin Pharmacokinet. 2012;51(3):147-62. doi: 10.2165/11598080-000000000-00000, PMID 22339447